

# Some multiquark potentials, pseudopotentials, and AdS/QCD

Oleg Andreev\*

*Technische Universität München, Excellence Cluster, Boltzmannstrasse 2, 85748 Garching, Germany*

(Received 7 May 2008; published 3 September 2008)

The static three-quark potential and pseudopotential of a pure  $SU(3)$  gauge theory are studied in a five-dimensional framework known as AdS/QCD. The results support the Y-ansatz for the baryonic area law. A comparison with the quark-antiquark calculations shows the universality of the string tension as well as the spatial string tension. We also discuss extensions to  $SU(N)$  gauge theories.

DOI: [10.1103/PhysRevD.78.065007](https://doi.org/10.1103/PhysRevD.78.065007)

PACS numbers: 12.39.Pn, 12.90.+b

## I. INTRODUCTION

Heavy-quark potentials are of primary importance in studying the mass spectra of mesons and baryons. They have been computed in lattice simulations, and the results reveal a remarkable agreement with phenomenology.<sup>1</sup>

Until recently, the lattice formulation even struggling with limitations and systematic errors was the main computational tool to deal with strongly coupled gauge theories. The situation changed drastically with the invention of the anti-de Sitter/conformal field theories (AdS/CFT) correspondence that resumed interest in finding a string description of strong interactions.

In this paper we continue a series of studies [2–4] devoted to the heavy-quark potentials and pseudopotentials within a five-dimensional framework nowadays known as AdS/QCD. In [2], the model was presented for computing the quark-antiquark potential. The resulting potential is Coulomb-like at short distances and linear at long range. Subsequent work [5] has made it clear that the model should be taken seriously, particularly in the context of consistency with the available lattice data as well as phenomenology. In [3,4], the models were presented for computing the quark-antiquark pseudopotentials resulting from the spatial Wilson loops. The results obtained for the spatial string tensions are remarkably consistent with the available lattice data for temperatures up to  $3T_c$ .

The question naturally arises: What happens when these models are used for computing multiquark potentials or pseudopotentials? The multiquark potentials have recently been the object of numerical studies.<sup>2</sup> In the case of great interest, three-quark states in a  $SU(3)$  gauge theory, the potential is well described by a simple model [8]

$$V_{3q} = -\alpha_{3q} \sum_{i<j}^3 \frac{1}{L_{ij}} + \sigma_{3q} L_{\min} + C. \quad (1.1)$$

Here  $C$  is a constant. The quarks form a triangle with sides of lengths  $L_{ij}$ .  $L_{\min}$  is the minimal length of the string

\*Also at Landau Institute for Theoretical Physics, Moscow.

<sup>1</sup>For a review, see [1].

<sup>2</sup>For reviews, see [6,7] and references therein.

network which has a junction at the Fermat point of the triangle [9]. Thus, the potential is given by the sum of the Coulomb terms and the linear term called the Y-law. A remarkable fact is that  $\sigma_{3q}$  is equal to  $\sigma_q$  found from the quark-antiquark potential. This is obvious in the string picture, where the string tension is universal, but it is far from being so in the lattice formulation.

The purpose of the present paper is two-fold. First, we examine the multiquark potentials that may also be thought of as a further cross-check of the model [2]. Second, we make a similar analysis of the multiquark pseudopotentials. To our knowledge, there have been no studies (numerical or analytical) of this problem in the literature.

The paper is organized as follows. In section II, we discuss the multiquark potentials. We begin with the three-quark potential. In this case, we demonstrate the Y-law and the universality of the string tension. Finally, we extend our analysis to the  $SU(N)$  case. We then go on in Sec. III to discuss the multiquark pseudopotentials. Here we also demonstrate the Y-law, the universality of the spatial string tension, and possible generalizations to  $SU(N)$ . We conclude in Sec. IV with a brief discussion of possibilities for further study. Some technical details are given in the appendix.

## II. CALCULATING THE POTENTIALS

In this section, we will discuss static multiquark potentials. We start with the three-quark potential in a  $SU(3)$  gauge theory, where equations are most elementary. In Sec. IID, similar issues are considered in the context of a  $SU(N)$  gauge theory.

### A. General formalism

As for the quark-antiquark potential, the static three-quark potential can be determined from the expectation value of a Wilson loop. The baryonic loop is defined in a gauge-invariant manner as  $W_{3q} = \frac{1}{3!} \varepsilon_{abc} \varepsilon_{a'b'c'} U_1^{aa'} U_2^{bb'} U_3^{cc'}$ , with the path-ordered exponents  $U_i$  along the lines shown in Fig. 1.

In the limit  $T \rightarrow \infty$  the expectation value of the Wilson loop is

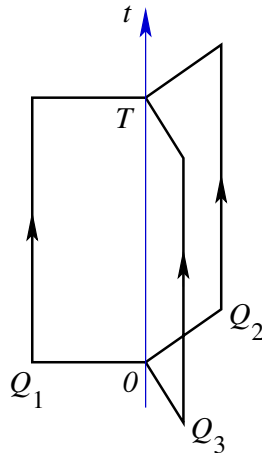


FIG. 1 (color online). A baryonic Wilson loop  $W_{3q}$ . A three-quark state is generated at  $t = 0$  and is annihilated at  $t = T$ . The quarks are spatially fixed in  $\mathbf{R}^3$  at points  $Q_1$ ,  $Q_2$ , and  $Q_3$ .

$$\langle W_{3q} \rangle \sim e^{-TV_{3q}}, \quad (2.1)$$

where  $V_{3q}$  is the three-quark potential.

In discussing baryonic Wilson loops, we adapt a formalism proposed within the AdS/CFT correspondence [10,11] to AdS/QCD.<sup>3</sup> So, we place heavy quarks at the boundary points of the five-dimensional space and consider a configuration in which each of the quarks is the endpoint of a fundamental string, with all the strings oriented in the same way. The strings join at a baryon vertex in the interior as shown in Fig. 2.<sup>4</sup> We also assume that the quarks form a triangle  $Q_1Q_2Q_3$  such that all the internal angles are smaller than  $\frac{2\pi}{3}$ .

Before proceeding to the detailed analysis, let us set the five-dimensional geometry. We consider the following deformation of the Euclidean AdS<sub>5</sub> [2,14]:

$$ds^2 = R^2 w(dt^2 + d\vec{x}^2 + dr^2), \quad w(r) = \frac{e^{\tilde{s}r^2}}{r^2}, \quad (2.2)$$

where  $d\vec{x}^2 = dx^2 + dy^2 + dz^2$  and  $\tilde{s}$  is a free parameter.<sup>5</sup> We also take a constant dilaton and discard other background fields.

The action of the system has in addition to the standard Nambu-Goto actions of the fundamental strings also a contribution arising from the baryon vertex. It is thus

<sup>3</sup>For subsequent developments of the formalism, see [12,13].

<sup>4</sup>From the point of view of ten-dimensional string theory, the baryon vertex is a wrapped five-brane whose world volume is  $\mathbf{R} \times \mathbf{X}$ , with  $\mathbf{X}$  a five-dimensional compact space and  $\mathbf{R}$  a timelike curve in AdS<sub>5</sub> or its deformed version, [10,11]. In AdS/QCD, it is reduced to a zero-brane (point).

<sup>5</sup>The value of  $\tilde{s}$  can be fixed, for example, from the quark-antiquark potential.

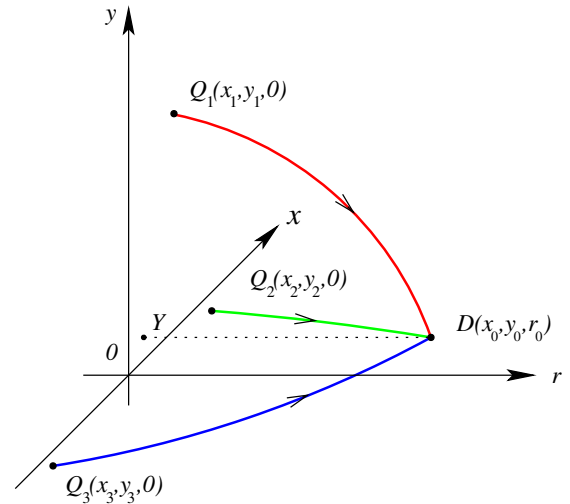


FIG. 2 (color online). A configuration used to calculate the expectation value of  $W_{3q}$ . The quarks are set on the  $x$ - $y$  plane. The baryon vertex is placed at  $D$ . Its projection on the  $x$ - $y$  plane is  $Y$ .

$$\mathcal{S} = \sum_{i=1}^3 S_i + S_{\text{vert}}, \quad (2.3)$$

where  $S_i$  denotes the action of the string connecting the  $i$ -quark with the vertex.

Like in the case of the quark-antiquark potential, a natural proposal for the expectation value of the Wilson loop is

$$\langle W_{3q} \rangle \sim e^{-\mathcal{S}_{\text{min}}}, \quad (2.4)$$

where  $\mathcal{S}_{\text{min}}$  is the minimal action of the system.

Since we are interested in a static configuration, we take

$$t_i(\tau_i) = \tau_i, \quad y_i(\sigma_i) = a_i \sigma_i + b_i. \quad (2.5)$$

Here  $(\tau_i, \sigma_i)$  are worldsheet coordinates. The action of the  $i$ -string is then

$$S_i = Tg \int_0^1 d\sigma_i w \sqrt{a_i^2 + x_i'^2 + r_i'^2}, \quad (2.6)$$

where  $g = \frac{R^2}{2\pi\alpha'}$ . A prime denotes a derivative with respect to  $\sigma_i$ .

The action for the baryon vertex is taken to be of the form

$$S_{\text{vert}} = T\mathcal{V}(r_0), \quad (2.7)$$

where  $\mathcal{V}$  can be considered as an effective potential of the vertex. Unfortunately, the explicit form of  $\mathcal{V}$  is not determined only from the five-dimensional metric (2.2). It requires the knowledge of the string theory dual to QCD. We will return to this issue in the next section.

The boundary conditions on the fields are given by

$$\begin{aligned} x_i(0) &= x_i, & y_i(0) &= y_i, & r_i(0) &= 0, \\ x_i(1) &= x_0, & y_i(1) &= y_0, & r_i(1) &= r_0. \end{aligned} \quad (2.8)$$

These determine the coefficients  $a_i$  and  $b_i$  in (2.5). Thus, we have

$$a_i = y_0 - y_i, \quad b_i = y_i. \quad (2.9)$$

Next, we extremize the total action  $\mathcal{S}$  with respect to the worldsheet fields  $x_i(\sigma_i)$  and  $r_i(\sigma_i)$  describing the strings as well as with respect to  $x_0, y_0$ , and  $r_0$  describing the location of the baryon vertex, with the following identifications:  $\delta x_i(1) = \delta x_0$  and  $\delta r_i(1) = \delta r_0$ . In doing so, we use the fact that there are two symmetries which simplify the further analysis.

Since the integrand in (2.6) does not depend explicitly on  $\sigma_i$ , we get the first integral of Euler-Lagrange equations

$$I_i = \frac{w_i}{\sqrt{a_i^2 + x_i'^2 + r_i'^2}}. \quad (2.10)$$

In addition, because of translational invariance along the  $x$ -direction, there is another first integral. Combining it with (2.10) gives

$$P_i = x_i'. \quad (2.11)$$

Together with the boundary conditions these equations determine  $x_i$

$$x_i(\sigma_i) = (x_0 - x_i)\sigma_i + x_i. \quad (2.12)$$

Now, we extremize the action with respect to the location of the baryon vertex. After using (2.9) and (2.12), we get

$$\begin{aligned} \sum_{i=1}^3 \frac{x_0 - x_i}{l_i \sqrt{1 + k_i}} &= 0, & \sum_{i=1}^3 \frac{y_0 - y_i}{l_i \sqrt{1 + k_i}} &= 0, \\ \sum_{i=1}^3 \frac{1}{\sqrt{1 + k_i^{-1}}} + \frac{1}{g} \frac{\mathcal{V}'}{w}(r_0) &= 0. \end{aligned} \quad (2.13)$$

Here  $k_i = \left(\frac{r_i(0)}{l_i}\right)^2$  and  $l_i = |YQ_i| = \sqrt{(x_0 - x_i)^2 + (y_0 - y_i)^2}$ .

If we define the first integrals  $I_i$  at  $\sigma_i = 1$  such that  $I_i = \omega(r_0)/l_i \sqrt{1 + k_i}$ , and then integrate over  $[0, 1]$  of  $d\sigma_i$ , then by virtue of (2.10) we get

$$\begin{aligned} l_i &= \sqrt{\frac{\lambda}{\tilde{g}(1 + k_i)}} \int_0^1 dv_i v_i^2 e^{\lambda(1-v_i^2)} \\ &\times \left(1 - \frac{1}{1 + k_i} v_i^4 e^{2\lambda(1-v_i^2)}\right)^{-1/2}, \end{aligned} \quad (2.14)$$

where  $v_i = r_i/r_0$  and  $\lambda = \tilde{g}r_0^2$ .

Now, we will compute the energy of the configuration. First, we reduce the integrals over  $\sigma_i$  in Eq. (2.6) to that

over  $r_i$ . This is easily done by using the first integral (2.10). Since the integral is divergent at  $r_i = 0$ , we regularize it by imposing a cutoff  $\epsilon$ . Then we replace  $r_i$  with  $v_i$  as in (2.14). Finally, the regularized expression takes the form

$$\begin{aligned} E_R &= \mathcal{V}(\lambda) + g \sqrt{\frac{\tilde{g}}{\lambda}} \sum_{i=1}^3 \int_{\sqrt{(\lambda/\tilde{g})\epsilon}}^1 \frac{dv_i}{v_i^2} e^{\lambda v_i^2} \\ &\times \left(1 - \frac{1}{1 + k_i} v_i^4 e^{2\lambda(1-v_i^2)}\right)^{-1/2}. \end{aligned} \quad (2.15)$$

Its  $\epsilon$ -expansion is

$$E_R = \frac{3g}{\epsilon} + O(1).$$

Subtracting the  $\frac{1}{\epsilon}$  term (quark masses) and letting  $\epsilon = 0$ , we find a finite result

$$\begin{aligned} E &= \mathcal{V}(\lambda) + g \sqrt{\frac{\tilde{g}}{\lambda}} \sum_{i=1}^3 \int_0^1 \frac{dv_i}{v_i^2} \\ &\times \left[ e^{\lambda v_i^2} \left(1 - \frac{1}{1 + k_i} v_i^4 e^{2\lambda(1-v_i^2)}\right)^{-1/2} - 1 - v_i^2 \right] \\ &+ C, \end{aligned} \quad (2.16)$$

where  $C$  stands for a normalization constant.

In contrast to the quark-antiquark case, the potential in question is more involved. It is given by a set of equations. Formally, one can eliminate parameters and find  $E$  as a function of the  $l_i$ 's or the  $L_{ij}$ 's. Unfortunately, in practice it is extremely difficult.

## B. A concrete example

We will next describe a concrete example in which one can develop a level of understanding that is somewhat similar to that of the quark-antiquark case [2]. We consider the most symmetric configuration of the quarks, in which the triangle  $Q_1Q_2Q_3$  is equilateral, and specify the action  $S_{\text{vert}}$  as that of a particle in a curved space. The latter implies that

$$\mathcal{V}(r_0) = mR\sqrt{\omega(r_0)}, \quad (2.17)$$

where  $m$  is a parameter, which can be interpreted as a mass of a "particle."

A consequence of the symmetry is that  $Y$ , which is the projection of  $D$  on the  $x$ - $y$  plane, is nothing but the circumcenter of the triangle  $Q_1Q_2Q_3$ . The first two equations of (2.13) are now identically satisfied, while the last takes the form<sup>6</sup>

<sup>6</sup>This equation determines the location of the vertex in the  $r$ -direction, because the symmetry argument alone is not enough to do so.

$$\frac{1}{\sqrt{1+k^{-1}}} = \kappa(1-\lambda)e^{-(1/2)\lambda}, \quad (2.18)$$

where  $k = k_i$  and  $\kappa = \frac{1}{3} \frac{mR}{g}$ .

With the form (2.18),  $k$  can be explicitly computed as a function of  $\lambda$ . Inserted in (2.14) and (2.16), this gives

$$l = \sqrt{\frac{\lambda}{\xi}} \rho \int_0^1 dv v^2 e^{\lambda(1-v^2)} \left(1 - \rho v^4 e^{2\lambda(1-v^2)}\right)^{-1/2} \quad (2.19)$$

and

$$E = 3g \sqrt{\frac{\xi}{\lambda}} \left[ \kappa e^{(1/2)\lambda} + \int_0^1 \frac{dv}{v^2} \left( e^{\lambda v^2} (1 - \rho v^4 e^{2\lambda(1-v^2)})^{-1/2} - 1 - v^2 \right) \right] + C, \quad (2.20)$$

where  $\rho(\lambda) = 1 - \kappa^2(1-\lambda)^2 e^{-\lambda}$ .

The potential in question is written in parametric form given by Eqs. (2.19) and (2.20).<sup>7</sup> It is unclear to us how to eliminate the parameter  $\lambda$  and find  $E$  as a function of  $l$ . We can, however, gain some important insights into the problem from two limiting cases as well as numerical calculations.

We start by noting that Eq. (2.18) makes sense only if  $\lambda < 1$ . This means that  $r_0$  must obey

$$r_0 \leq \sqrt{\frac{1}{\xi}}. \quad (2.21)$$

So in other words, the baryon vertex is prevented from getting deeper into the  $r$ -direction. This gives a kind of wall which is a generic feature of confining theories. It is worth mentioning that the same upper bound was found in the quark-antiquark case [2] by inspecting the integral (2.19) at  $\rho = 1$ . The point is that the integral is real for  $\lambda < 1$ . It develops a logarithmic singularity at  $\lambda = 1$  and becomes complex for larger  $\lambda$ . A similar analysis shows that if  $\kappa \leq 1$  this holds for smaller  $\rho$  too. For  $\kappa > 1$  things are more subtle because of a lower bound

$$r_* \leq r_0. \quad (2.22)$$

Here  $r_*$  is a root of  $\rho(\xi r^2) = 0$ . The physical reason for this is a big mass of the particle that strengthens a gravitational force pushing the baryon vertex deeper into the interior. As a result, for small  $l$  the configuration looks like a spike of height  $r_*$ .

The fact that both the Eqs. (2.18) and (2.19) lead to the same upper bound suggests that neither strings nor baryon vertices are allowed to get deeper into the  $r$ -direction than

<sup>7</sup>Note that these equations are reduced to those of [2] at  $\kappa = 0$  and  $\rho = 1$ .

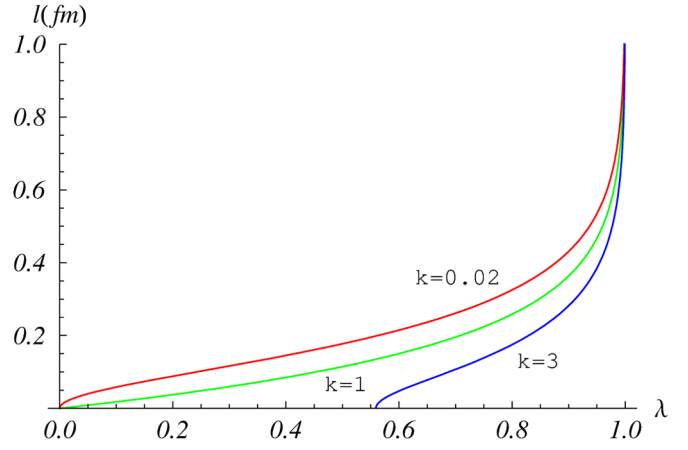


FIG. 3 (color online). Plots of  $l(\lambda, \kappa)$  for fixed  $\kappa$ . Here  $\xi = 0.45 \text{ GeV}^2$ .

$1/\sqrt{\xi}$ . This seems natural enough from the point of view of consistency.

To complete the picture, let us present the results of numerical calculations. The parametric Eq. (2.19) predicts a characteristic form of  $l$ , as shown in Fig. 3. We see that the curves behave similarly in the vicinity of  $\lambda = 1$  but rather differently for smaller  $\lambda$ . This has an interesting effect on the form of the interquark potential, as we will see in a moment.

Having understood the correspondence between  $\lambda$  and  $l$ , we can investigate the properties of the interquark interaction at long and short distances.<sup>8</sup>

At long distances the interquark interaction being independent of  $\kappa$  is given by

$$E = \sigma_{3q} L_{\min} + O(1) \quad (2.23)$$

that is nothing but the desired Y-law. Here  $L_{\min} = 3l$  and  $\sigma_{3q} = e g \xi$ .

Some comments about formula (2.23) are in order. First, the form of the potential is in agreement with both the old flux-tube picture of hadrons and more recent calculations in lattice QCD [6,7]. However, the key difference is that in our model the interaction takes place in the interior of five-dimensional space, whereas in those it happens on its boundary. Next, the tension  $\sigma_{3q}$  is the same as that found from the quark-antiquark potential [2]. Thus, the model also supports the universality of the string tension. Finally, to leading order the energy is the sum of the string contributions. A contribution from the baryon vertex appears at next-to-leading order.

At short distances the form of the interquark interaction depends on the value of  $\kappa$ . We have the Coulomb terms

$$E = -3 \frac{\alpha_{3q}}{L} + O(1), \quad (2.24)$$

<sup>8</sup>More details are presented in the appendix.

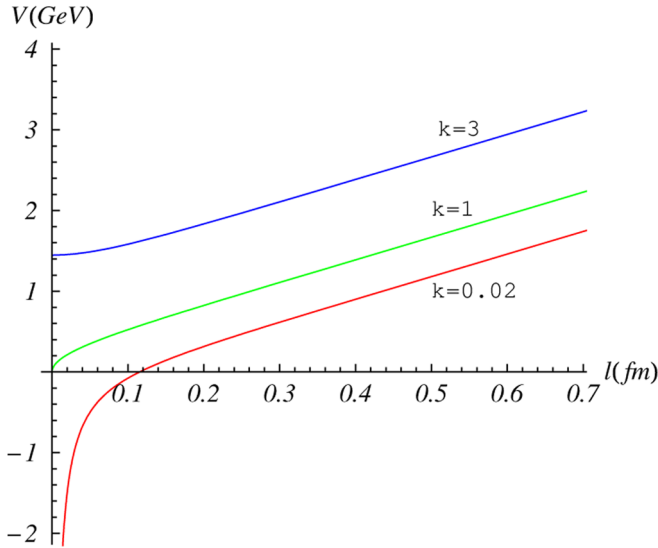


FIG. 4 (color online). Plots of  $E(l, \kappa)$  for fixed  $\kappa$ . We set  $g = 0.15$ ,  $\tilde{s} = 0.45 \text{ GeV}^2$ ,  $C = 0$ .

with  $L$  a distance between the quarks, if and only if  $\kappa < 1$ . In other cases, the energy behaves as  $E \sim \text{const}$ .

Just as in the examples discussed in the AdS/CFT formulation [10,12], in (2.24) the contribution of the baryon vertex is compatible to that of the strings. The reason for this is obvious: in the region of small  $r$  the metric (2.2) behaves asymptotically as Euclidean AdS<sub>5</sub>.

As an illustration, Fig. 4 shows the results of numerical calculations. We see that the value of  $\kappa$  does matter at short distances, while it becomes irrelevant at large distances.

We conclude this section by making a few estimates, which might be of interest for phenomenology.

As already noted, in AdS/CFT the baryon vertex is the wrapped five-brane. For definiteness, consider type IIB string theory on AdS<sub>5</sub> × S<sup>5</sup>. The D5 brane world volume is then S<sup>5</sup> × R, with R a timelike curve in AdS<sub>5</sub>. Now, suppose that the action of the brane is simply the Nambu-Goto term  $\tau_5 \int d^6 \xi \sqrt{g}$ , with  $\tau_5$  the tension.<sup>9</sup> In the static case this leads to the same form as (2.17). Moreover, we learn that  $\kappa = \frac{1}{4}$ .

At first sight, it seems reasonable to fix the value of  $\kappa$  by equating  $\alpha_{3q}$  and  $\frac{1}{2}\alpha_{q\bar{q}}$ .<sup>10</sup> A little experimentation with MATHEMATICA shows, however, that this results in a negative value. If we assume that  $\alpha_{3q} = Y\alpha_{q\bar{q}}$ , then there are positive  $\kappa$ 's for  $Y$ 's relatively close to 0.5, as given in Table I. Note that  $\kappa = \frac{1}{4}$  corresponds to  $Y = 0.27$  versus  $Y \approx 0.5$  in lattice QCD. It is possible to partially fix this discrepancy by choosing smaller  $\kappa$ . Then the value one needs are bounded from above by a number of order 0.02.

<sup>9</sup>The general form of the action is given by the DBI and WZ terms plus  $\alpha'$  corrections. See, e.g., [15].

<sup>10</sup>With accuracy better than a few percent, such a relation is valid in lattice QCD [8].

TABLE I. Estimates of the parameter  $\kappa$ .

	0.50	0.45	0.42	0.38	0.27
Y	0.50	0.45	0.42	0.38	0.27
$\kappa$	-0.11	-0.03	0.02	0.07	0.25

The problem is, of course, that the action for the baryon vertex we used in (2.17) is oversimplified. There are extra background scalars as well as  $\alpha'$  corrections.<sup>11</sup> However, there is also a possibility that the string formulation being reliable at large distances provides only a qualitative description of the physics at short distances.

### C. Y-law and string tension

Apparently, one of the requirements for the multiquark model should be consistency with the quark-antiquark case: as long as the fundamental strings are prevented from getting deeper into the  $r$ -direction, the baryon vertex, as a string endpoint, should also be prevented from doing so. Our next goal will be to understand the large distance behavior of the multiquark potential from this point of view.

To implement this approach, we assume that (1) the baryon potential  $\mathcal{V}(r_0)$  is a positive and regular function of  $r_0$  such that it reaches the minimum exactly at  $r_0 = 1/\sqrt{\tilde{s}}$ ; (2)  $\mathcal{V} \rightarrow +\infty$  as  $r_0$  tends to zero or infinity. The latter means that the vertex cannot come very close to the boundary as well as go far away from it.

These conditions allow us to conclude that the last equation of (2.13) makes sense only if  $r_0$  is subject to the constraint (2.22). We also learn that  $k_i \rightarrow 0$  as  $\lambda \rightarrow 1$ .

If we look at Eq. (2.14), then a short inspection shows that  $l_i$  takes large values only in the corner of the parameter space  $(k_i, \lambda)$  located at  $(0, 1)$ . In this region  $l_i$  behaves as

$$l_i = -\frac{1}{2}\sqrt{\frac{1}{\tilde{s}}}\ln(\sqrt{k_i} + 1 - \lambda) + O(1). \quad (2.25)$$

Note that in the symmetric case  $k_i \sim (1 - \lambda)^2$ . Hence, the equation reduces to (A1).

A precisely analogous computation for  $E$  gives

$$E = -\frac{1}{2}e g \sqrt{\tilde{s}} \sum_{i=1}^3 \ln(\sqrt{k_i} + 1 - \lambda) + O(1). \quad (2.26)$$

A contribution from the baryon vertex is of order 1, because the function  $\mathcal{V}$  is finite at  $\lambda = 1$ . Combining this with (2.25), we find the energy configuration as a function of the lengths  $l_i$

<sup>11</sup>In contrast to AdS/CFT, where  $\frac{\alpha'}{R^2} \sim \frac{1}{\sqrt{\lambda}}$ , becomes small for large 't Hooft coupling, the phenomenological estimate of [2] gives  $\frac{\alpha'}{R^2} \sim 1$ . The latter suggests that  $\alpha'$  corrections are relevant for the real world and a departure from the supergravity approximation is needed.

$$E = \sigma_{3q} \sum_{i=1}^3 l_i + O(1). \quad (2.27)$$

Here  $\sigma_{3q}$  is equal to  $\sigma_{q\bar{q}}$  of [2], as expected from the universality of the string picture.

However, this is not the whole story. We still need to show that  $Y$  is the Fermat point of the triangle formed by the quarks. The simplest way to see this is to take the limit  $k_i \rightarrow 0$  in the first two equations of (2.13) which determine the location of the vertex on the  $x$ - $y$  plane. We have thus

$$\sum_{i=1}^3 \frac{1}{l_i} (x_0 - x_i) = 0, \quad \sum_{i=1}^3 \frac{1}{l_i} (y_0 - y_i) = 0. \quad (2.28)$$

Obviously, these equations are a result of differentiating the sum  $\sum_{i=1}^3 l_i$  with respect to  $x_0$  and  $y_0$ . Because a solution

$$x_0 = \frac{1}{\mathcal{N}} \sum_{i=1}^3 \frac{x_i}{l_i}, \quad y_0 = \frac{1}{\mathcal{N}} \sum_{i=1}^3 \frac{y_i}{l_i}, \quad \mathcal{N} = \sum_{i=1}^3 \frac{1}{l_i} \quad (2.29)$$

determines the Fermat point, in this limit  $Y$  tends to the Fermat point of the triangle. This completes our derivation of the Y-law.

#### D. The case $SU(N)$

Now we consider the case  $SU(N)$ . The analysis is a little bit more complicated but the results are very similar.

By analogy with Sec. II A, we place  $N$  heavy quarks on the boundary of the five-dimensional space. Because in a generic case the quarks are not on the same plane, we need to involve the third spatial coordinate  $z$ . So, the quarks are fixed in  $\mathbf{R}^3$  at points  $Q_i$  with coordinates  $x_i, y_i, z_i$ . The configuration of interest is constructed as the  $N$  quarks joined together by the  $N$  fundamental strings ending at the baryon vertex in the interior of the five-dimensional space whose metric takes the form (2.2).

The total action of the system is given by (2.3), where the sum now runs from 1 to  $N$ . After choosing the gauge (2.5), the action of the  $i$ -string takes the form

$$S_i = Tg \int_0^1 d\sigma_i w \sqrt{a_i^2 + x_i'^2 + z_i'^2 + r_i'^2}. \quad (2.30)$$

The boundary conditions are given by Eq. (2.8) together with

$$z_i(0) = z_i, \quad z_i(1) = z_0. \quad (2.31)$$

In addition to the first integrals of Sec. II A, which correspond to Euler-Lagrange equations for the fields  $x_i(\sigma_i)$  and  $r_i(\sigma_i)$ , there is one more integral due to translational invariance in the  $z$ -direction. Combining it with (2.10) results in

$$\bar{P}_i = z_i'. \quad (2.32)$$

These equations yield solutions

$$z_i(\sigma_i) = (z_0 - z_i)\sigma_i + z_i \quad (2.33)$$

which coincide at the endpoints with the boundary values defined in (2.31).

Extremizing the action with respect to the location of the vertex, we get (2.13), with the upper bound of summation given by  $N$ , and

$$\sum_{i=1}^N \frac{z_0 - z_i}{l_i \sqrt{1 + k_i}} = 0 \quad (2.34)$$

that determines the location of the baryon vertex along the  $z$ -direction. Note that now  $l_i = \sqrt{(x_0 - x_i)^2 + (y_0 - y_i)^2 + (z_0 - z_i)^2}$ .

Like in the case  $N = 3$ , we can compute the expressions for the lengths  $l_i$ . After doing so, we find that they take the forms as in (2.14) and (2.16), with the only difference:  $E$  now includes the contributions from the  $N$  fundamental strings.

It is also straightforward to extend the analysis of Sec. II C to the case of interest. Assuming the same form of  $\mathcal{V}$ , we quickly come to similar conclusions about the bound (2.21) and large values of  $l_i$ . Continuing along those lines leads to the asymptotic behaviors as (2.25) and (2.26). Finally, we get

$$E = \sigma_{Nq} \sum_{i=1}^N l_i + O(1). \quad (2.35)$$

As before the string tension  $\sigma_{Nq}$  is equal to that of the quark-antiquark case.

To complete the picture, we should check that  $E$  given by the above formula is minimum. The essential point is to take the limit  $k_i \rightarrow 0$  in the equations determining the vertex location. Then, from Eqs. (2.28) and

$$\sum_{i=1}^N \frac{1}{l_i} (z_0 - z_i) = 0, \quad (2.36)$$

we learn that  $Y$  is nothing but the geometric median of the set of the points  $Q_i$ .<sup>12</sup> This is the desired result which reflects the fact that  $E$  is minimum.

### III. CALCULATING THE PSEUDOPOTENTIALS

In this section we will investigate the temperature dependence of the spatial string tension. The model of interest is developed for the quark-antiquark case in [3,4], to which the reader is referred for more details. The philosophy is that the spatial string tension is determined from temperature dependent pseudopotentials extracted from the spatial Wilson loops.<sup>13</sup>

<sup>12</sup>It is also known as the Fermat-Weber point. See, e.g., [16].

<sup>13</sup>These are Wilson loops in hyperplanes orthogonal to the temporal direction.

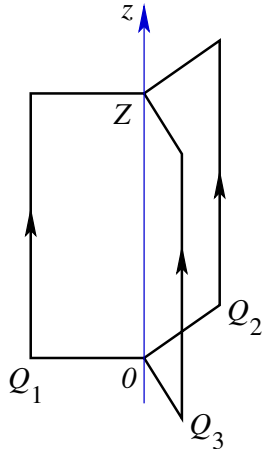


FIG. 5 (color online). A baryonic spatial Wilson loop  $W_{3q}$ . The points  $Q_i$  are on the  $x$ - $y$  plane.

### A. General formalism

As before, we begin with the case  $SU(3)$ . Let  $\tilde{W}_{3q}$  be a spatial Wilson loop in  $\mathbf{R}^3$ , at a fixed value of  $t$ , with the path-ordered exponents  $U_i$  along the lines shown in Fig. 5.

In the limit  $Z \rightarrow \infty$  the expectation value of the loop is given by

$$\langle \tilde{W}_{3q} \rangle \sim e^{-Z\tilde{V}_{3q}}, \quad (3.1)$$

where  $\tilde{V}_{3q}$  is a pseudopotential.

Following [3,4], we take the following ansatz for the five-dimensional geometry which turned out to be quite successful in the quark-antiquark case

$$ds^2 = R^2 w (f dt^2 + d\vec{x}^2 + f^{-1} dr^2), \quad f = 1 - \frac{r^4}{r_T^4}, \quad (3.2)$$

where  $r_T = 1/\pi T$ . Note that it is nothing but a deformation of the black hole in  $AdS_5$ .

To compute the spatial loop in question, we study a configuration similar to that shown in Fig. 2: three fundamental strings, with the same orientation, such that the  $i$ -string begins at  $Q_i$  and ends on the baryon vertex in the interior. The total action of the system is then given by the sum of the string actions and the action for the vertex. Because we are interested in the configuration independent of  $z$ , for the worldsheet coordinates we can choose

$$z_i(\tau_i) = \tau_i, \quad y_i(\sigma_i) = a_i \sigma_i + b_i. \quad (3.3)$$

With such a choice, the action of the  $i$ -string is then

$$S_i = Z g \int_0^1 d\sigma_i w \sqrt{a_i^2 + x_i'^2 + f^{-1} r_i'^2}. \quad (3.4)$$

As before, for the baryon vertex we take the action of the form

$$S_{\text{vert}} = Z \mathcal{V}(r_0). \quad (3.5)$$

The boundary conditions on the fields are given by (2.8). These determine the coefficients  $a_i$  and  $b_i$  in (3.3).

To find the configuration, we must extremize the total action with respect to the worldsheet fields  $x_i(\sigma_i)$  and  $r_i(\sigma_i)$  as well as with respect to the coordinates of the vertex  $x_0, y_0, r_0$ . The underlying symmetries of the model provide a couple of first integrals that simplify the analysis. Since the integrand in (3.4) does not depend explicitly on  $\sigma_i$ , we have an integral

$$J_i = \frac{w_i}{\sqrt{a_i^2 + x_i'^2 + f^{-1} r_i'^2}}. \quad (3.6)$$

Like in Sec. II A, translational invariance along the  $x$ -direction yields another integral. Combining it with (3.6) results in (2.11). Once this integral has been found, the  $x_i$ 's can be determined. As a result, we obtain (2.12).

Now, we extremize the action with respect to the location of the baryon vertex. At finite temperature, Eqs. (2.13) are changed as follows. There is a factor  $f^{-1}$  in front of  $k_i$ . Explicitly,

$$\begin{aligned} \sum_{i=1}^3 \frac{x_0 - x_i}{l_i \sqrt{1 + f_0^{-1} k_i}} &= 0, & \sum_{i=1}^3 \frac{y_0 - y_i}{l_i \sqrt{1 + f_0^{-1} k_i}} &= 0, \\ \sum_{i=1}^3 \frac{1}{\sqrt{f_0^{-1} + k_i^{-1}}} + \frac{1}{g} \frac{f_0}{w} \mathcal{V}'(r_0) &= 0, \end{aligned} \quad (3.7)$$

where  $f_0 = 1 - \frac{r_0^4}{r_T^4}$ . By virtue of (3.6), the integral over  $[0, 1]$  of  $\sigma_i$  is equal to

$$\begin{aligned} l_i &= \sqrt{\frac{\lambda}{\tilde{s}(1 + f_0^{-1} k_i)}} \int_0^1 dv_i v_i^2 e^{\lambda(1-v_i^2)} \left(1 - \left(\frac{\lambda}{\tilde{s} r_T^2}\right)^2 v_i^4\right)^{-1/2} \\ &\times \left(1 - \frac{1}{1 + f_0^{-1} k_i} v_i^4 e^{2\lambda(1-v_i^2)}\right)^{-1/2}. \end{aligned} \quad (3.8)$$

Here we have expressed the integration constant via the values of the fields at  $\sigma_i = 1$ .

Now we will present an expression for the energy (pseudopotential) of the configuration. The computation is just as above.<sup>14</sup> At the end of the day, we have

$$\begin{aligned} \tilde{E} &= \mathcal{V}(\lambda) + g \sqrt{\frac{\tilde{s}}{\lambda}} \sum_{i=1}^3 \int_0^1 \frac{dv_i}{v_i^2} \left[ e^{\lambda v_i^2} \left(1 - \left(\frac{\lambda}{\tilde{s} r_T^2}\right)^2 v_i^4\right)^{-1/2} \right. \\ &\times \left. \left(1 - \frac{1}{1 + f_0^{-1} k_i} v_i^4 e^{2\lambda(1-v_i^2)}\right)^{-1/2} - 1 - v_i^2 \right] + C, \end{aligned} \quad (3.9)$$

<sup>14</sup>Indeed, our previous discussion in Sec. II A corresponds to the case  $f = 1$ .

where  $C$  is a normalization constant. As a result, the pseudopotential is given in parametric form by Eqs. (3.7), (3.8), and (3.9).

### B. Y-law and spatial string tension

Now we consider the analog of the Y-law for the pseudopotentials. For this, we continue to assume that  $\mathcal{V}(r_0)$  is a positive and regular function with a minimum at  $r_0 = 1/\sqrt{\tilde{s}}$  and singularities at the endpoints.

For this choice of  $\mathcal{V}$ , we can now determine the allowed values of  $r_0$ . A simple analysis shows that Eqs. (3.7) are consistent if  $r_0 < \min(1/\sqrt{\tilde{s}}, r_T)$  or  $r_0 > \max(1/\sqrt{\tilde{s}}, r_T\sqrt{1+k_i})$ . Since the latter yields complex values of  $l_i$ , it must be omitted. We have thus

$$r_0 \leq \min(1/\sqrt{\tilde{s}}, r_T). \quad (3.10)$$

What we have found is nothing but the bound of [3,4]. In addition to (2.22), it now states that neither strings nor baryon vertices may go behind the horizon ( $r = r_T$ ). From the point of view from [3], the bound gives rise to the two walls: (1) If  $1/\sqrt{\tilde{s}} < r_T$ , then the first wall,  $r_0 = 1/\sqrt{\tilde{s}}$ , dominates. This is interpreted as the low temperature phase. (2) If  $r_T < 1/\sqrt{\tilde{s}}$ , then the second wall,  $r_0 = r_T$ , dominates. This is the high temperature phase. The phase transition point is at  $r_T = 1/\sqrt{\tilde{s}}$ . In terms of a critical temperature and the parameter  $\tilde{s}$ , it is written as

$$T_c = \frac{1}{\pi} \sqrt{\tilde{s}}. \quad (3.11)$$

Having determined the allowed region for the parameter  $r_0$ , we are now ready to study  $l_i$  as a function of two variables. To this end, we look for level curves in the allowed region.<sup>15</sup> A summary of our numerical results is shown in Fig. 6. The first observation is that  $l_i$  takes large values only in the vicinity of the lower right corner which lies on the  $\lambda$  axis at  $\lambda = 1$  if  $T < T_c$  and at  $\lambda = \tilde{s}r_T^2$  if  $T > T_c$ . Another important point is that at nonzero  $k_i$  the length  $l_i$  vanishes at  $f = 0$ . This fact implies that in the high temperature phase we should keep  $k_i/f_0 \rightarrow 0$  to get large lengths.

According to the numerical analysis,  $l_i$  may become large only if  $k_i$  is small and  $r_0$  saturates the bound (3.10). It follows from (3.8) and (3.9), that in this limit the length and the energy behave as

$$l_i = -\frac{1}{2} \sqrt{\frac{\lambda}{\tilde{s}}} \ln(\beta\sqrt{k_i} + k_i f_0^{-1}(1-f_0) + f_0(1-\lambda))^{1/\beta} + O(1), \quad (3.12)$$

<sup>15</sup>As an illustration, we take  $k_i \leq 2$ . We do not elaborate on upper bounds for the  $k_i$ 's, because it is irrelevant for our purposes.

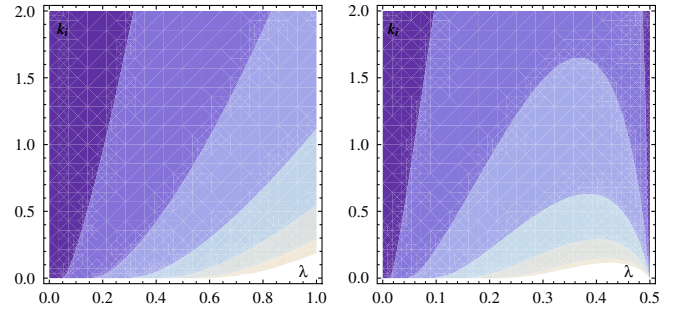


FIG. 6 (color online). Level curves for  $l_i = r(\lambda, k_i)$ : in the low temperature phase (left) at  $T = T_c/\sqrt{2}$  and in the high temperature phase (right) at  $T = \sqrt{2}T_c$ . Larger values are shown lighter. Here  $\tilde{s} = 0.45 \text{ GeV}^2$ .

$$\tilde{E} = -\frac{1}{2} g e^\lambda \sqrt{\frac{\tilde{s}}{\lambda}} \sum_{i=1}^3 \ln(\beta\sqrt{k_i} + k_i f_0^{-1}(1-f_0) + f_0(1-\lambda))^{1/\beta} + O(1), \quad (3.13)$$

where  $\beta^2 = 4 - \frac{3}{2}k_i f_0^{-1} + \frac{3}{2}k_i - \frac{11}{2}f_0 + \frac{1}{2}\lambda(17f_0 - 8) - 2\lambda^2 f_0$ . From these formulas, it is evident that at large distances the pseudopotential is given by

$$\tilde{E} = \tilde{\sigma}_{3q} \sum_{i=1}^3 l_i + O(1), \quad (3.14)$$

with the spatial tension

$$\tilde{\sigma}_{3q} = \begin{cases} \sigma_{3q} & \text{if } T \leq T_c, \\ \sigma_{3q} \left(\frac{T}{T_c}\right)^2 \exp\left\{\left(\frac{T}{T_c}\right)^2 - 1\right\} & \text{if } T \geq T_c. \end{cases} \quad (3.15)$$

Here,  $\sigma_{3q}$  is the physical tension at zero temperature. The temperature dependence of  $\tilde{\sigma}_{3q}$  is the same as that of [3,4] found in the quark-antiquark case. This suggests that the spatial string tension is also universal.

Finally, taking the limit  $k_i \rightarrow 0$  in the first two equations of (3.7), we learn that  $Y$  is the Fermat point of the triangle  $Q_1 Q_2 Q_3$ . Thus, we have derived, in the case of the pseudopotential, the Y-law analogous to that of the quark potentials.

### C. Further remarks

We have here considered the five-dimensional framework for studying the spatial string tension. However, if one can describe the string theory construction, this gives the baryon vertex as a wrapped five-brane. In this case, the brane world volume is  $\mathbf{R} \times \mathbf{X}$ , with  $\mathbf{R}$  a spacelike curve in the deformed  $\text{AdS}_5$ .

It is worth noting that the temperature dependence of the spatial tension is in good agreement with the lattice data for  $T \leq 3T_c$  [3,4]. Note that at higher temperatures it is determined by the  $\beta$ -function of a pure  $SU(3)$  gauge theory [17]. Clearly, our model cannot reproduce logarithms as-



sociated with the running coupling. Instead, it provides a complementary description in the strong coupling regime.

The above analysis can be easily generalized to the case  $SU(N)$ . Compared to the discussion of Sec. II D, the points  $Q_i$  are now on the  $x$ - $y$  plane. Hence, we need not involve any additional coordinate. The formal modification to be made is to extend the upper bound of summation to  $N$ . Thus, the temperature dependence of the spatial string tension is given by (3.15) that is the desired result [4].

#### IV. CONCLUDING COMMENTS

We have so far discussed the configurations including a single baryon vertex. In general, it is possible to consider configurations with an arbitrary number of vertices: string networks.

To give an idea of how this works, let us consider, though only schematically, the tetraquark case that is the four-quark potential  $V_{4q}$ . We place quarks and antiquarks at boundary points  $Q_i$  and  $\bar{Q}_i$ , respectively. These points are endpoints of fundamental strings. There are two basic configurations, as sketched in Fig. 7. The connected configuration includes five strings beginning at the boundary points and ending on the baryon and antibaryon vertices in the interior of the five-dimensional space. The disconnected configuration, a “two-meson” state, includes two strings stretched between the quarks and antiquarks.

For the tetraquark potential, there is a well-known “flip-flop” [18]. When the quarks and antiquarks are well separated, the potential is given by Coulomb terms plus a term which indicates the formation of the two-Y flux. On the other hand, when the quarks and antiquarks are close, the potential becomes a sum of two quark-antiquark potentials. Clearly, these two possibilities correspond to our connected and disconnected configurations.

From the point of view of ten-dimensional string theory, it is very easy to understand why the disconnected configuration dominates at small separations. The connected configuration includes the baryon and antibaryon vertices that is nothing but a brane-antibrane system in ten dimensions. There is a critical separation for such a system. For smaller separations, the open string spectrum consists of a

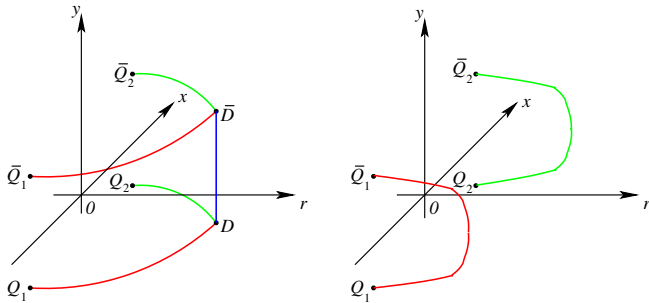


FIG. 7 (color online). Configurations used to calculate the tetraquark potential.

tachyon mode. The instability associated with the tachyon represents a flow toward annihilation of the brane-antibrane system.

#### ACKNOWLEDGMENTS

This work was supported in part by DFG “Excellence Cluster” and the Alexander von Humboldt Foundation under Grant No. PHYS0167. The author thanks G. Lopes Cardoso, D. Sorokin, V.I. Zakharov, and P. Weisz for discussions and comments.

#### APPENDIX

The purpose of this appendix is to consider the two limiting cases of Eqs. (2.19) and (2.20): short and long distances.

We begin with the case of long distances. As in Fig. 3, large  $l$ 's correspond to values of  $\lambda$  near 1. For  $\lambda \rightarrow 1$ , the integrals in (2.19) and (2.20) can be evaluated to give<sup>16</sup>

$$l = -\frac{1}{2}\sqrt{\frac{1}{\xi}}\ln(1-\lambda) + O(1), \quad (A1)$$

$$E = -\frac{3}{2}e\mathfrak{g}\sqrt{\xi}\ln(1-\lambda) + O(1).$$

Now, the parameter  $\lambda$  is easily eliminated, and one gets

$$E = \sigma_{3q}L_{\min} + O(1), \quad (A2)$$

where  $L_{\min} = 3l$  and  $\sigma_{3q} = e\mathfrak{g}\xi$ .

In a similar spirit, we can explore the short distance behavior of  $E$ . For  $\kappa \leq 1$ , this is simple because we need to take the limit  $\lambda \rightarrow 0$  (see Fig. 3). Expanding the right-hand sides of (2.19) and (2.20) in powers of  $\lambda$ , at leading order we obtain

$$l = \lambda^{1/2}(l_0 + O(\lambda)), \quad E = -\lambda^{-1/2}(E_0 + O(\lambda^{1/2})),$$

where  $l_0 = \sqrt{\frac{1-\kappa^2}{9\xi}}F_1[\frac{1}{2}, \frac{3}{4}; \frac{7}{4}; 1-\kappa^2]2$  and  $E_0 = 3\mathfrak{g}\sqrt{\xi}({}_2F_1[-\frac{1}{4}, \frac{1}{2}; \frac{3}{4}; 1-\kappa^2] - \kappa)$ . Combining these formulas, we find

$$E = -3\frac{\alpha_{3q}}{L} + O(1), \quad (A3)$$

where  $\alpha_{3q} = l_0E_0/\sqrt{3}$ .

The case  $\kappa = 1$  can be treated similarly. Our previous formulas for  $l$  and  $E$  become

$$l = l_1\lambda + O(\lambda^2), \quad E = C + E_1\lambda^{1/2} + O(\lambda^{3/2}),$$

where  $l_1 = 1/\sqrt{3\xi}$  and  $E_1 = 6\mathfrak{g}\sqrt{\xi}$ . This implies that

<sup>16</sup>The integrals are dominated by  $v \sim 1$ , where they take the form  $\int dv/\sqrt{a+b(1-v)+c(1-v)^2}$ . The remaining integral may be found in [19].

$$E = C + \gamma L^{1/2} + O(L), \quad (\text{A4})$$

where  $\gamma = E_1/\sqrt[3]{3l_1^2}$ .

For larger values of  $\kappa$ , the analysis is a bit more involved because of the lower bound (2.22). In this case we need to take the limit  $\lambda \rightarrow \lambda_*$  (see Fig. 3). Note that  $\rho(\lambda_*) = 0$ . A simple but somewhat tedious calculation shows that in the neighborhood of  $\lambda = \lambda_*$  the length  $l$  and the energy behave as

$$l = (\lambda - \lambda_*)^{1/2}(l_0^* + O(\lambda - \lambda_*)),$$

$$E = E_0^* + E_1^*(\lambda - \lambda_*) + O((\lambda - \lambda_*)^2),$$

with

$$l_0^* = \frac{1}{4} \sqrt{\frac{\rho'}{\xi \lambda_*}} \left( \sqrt{\frac{\pi}{\lambda_*}} \operatorname{erf}(\sqrt{\lambda_*}) - 2 \right), \quad E_0^* = E(\lambda_*),$$

$$E_1^* = \frac{3}{8} \xi \rho' e^{2\lambda_*} \sqrt{\frac{\xi}{\lambda_*^3}} \left( \sqrt{\frac{\pi}{\lambda_*}} \operatorname{erf}(\sqrt{\lambda_*}) - 2e^{-\lambda_*} \right).$$

Here  $\rho'$  denotes the derivative of  $\rho$  at  $\lambda = \lambda_*$ . This implies that at short distances the potential is given by

$$E = E_0^* + \gamma L^2 + O(L^3), \quad (\text{A5})$$

where  $\gamma = E_1^*/3(l_0^*)^2$ .

- 
- [1] G. S. Bali, Phys. Rep. **343**, 1 (2001).  
 [2] O. Andreev and V.I. Zakharov, Phys. Rev. D **74**, 025023 (2006).  
 [3] O. Andreev and V.I. Zakharov, Phys. Lett. B **645**, 437 (2007).  
 [4] O. Andreev, Phys. Lett. B **659**, 416 (2008).  
 [5] C.D. White, Phys. Lett. B **652**, 79 (2007); M. V. Carlucci, F. Giannuzzi, G. Nardulli, M. Pellicoro, and S. Stramaglia, arXiv:0711.2014.  
 [6] Ph. de Forcrand and O. Jahn, Nucl. Phys. **A755**, 475 (2005).  
 [7] H. Suganuma, A. Yamamoto, N. Sakumichi, T. Takahashi, H. Iida, and F. Okiharu, arXiv:0802.3500.  
 [8] T.T. Takahashi, H. Matsufuru, Y. Nemoto, and H. Suganuma, Phys. Rev. Lett. **86**, 18 (2001).  
 [9] See, e.g., [http://en.wikipedia.org/wiki/Fermat\\_point](http://en.wikipedia.org/wiki/Fermat_point).  
 [10] E. Witten, J. High Energy Phys. 07 (1998) 006.  
 [11] D.J. Gross and H. Ooguri, Phys. Rev. D **58**, 106002 (1998).  
 [12] A. Brandhuber, N. Itzhaki, J. Sonnenschein, and S. Yankielowicz, J. High Energy Phys. 07 (1998) 020.  
 [13] C. Athanasiou, H. Liu, and K. Rajagopal, J. High Energy Phys. 05 (2008) 083.  
 [14] O. Andreev, Phys. Rev. D **73**, 107901 (2006).  
 [15] J. Polchinski, *String Theory* (Cambridge University Press, Cambridge, England, 1998), Vol. II.  
 [16] See, e.g., [http://en.wikipedia.org/wiki/Geometric\\_median](http://en.wikipedia.org/wiki/Geometric_median).  
 [17] G. Boyd, J. Engels, F. Karsch, E. Laermann, C. Legeland, M. Lutgemeier, and B. Petersson, Phys. Rev. Lett. **75**, 4169 (1995).  
 [18] For a discussion and references, see, e.g., F. Okiharu, H. Suganuma, and T.T. Takahashi, Phys. Rev. D **72**, 014505 (2005).  
 [19] I.S. Gradshteyn and I.M. Ryzhik, *Table of Integrals, Series, and Products* (Academic Press, New York, 1994).